

# SASG-DA: Sparse-Aware Semantic-Guided Diffusion Augmentation For Myoelectric Gesture Recognition

Chen Liu, Can Han, Weishi Xu, Yaqi Wang, and Dahong Qian, *Senior Member, IEEE*

**Abstract**—Surface electromyography (sEMG)-based gesture recognition plays a critical role in human-machine interaction (HMI), particularly for rehabilitation and prosthetic control. However, sEMG-based systems often suffer from the scarcity of informative training data, leading to overfitting and poor generalization in deep learning models. Data augmentation offers a promising approach to increasing the size and diversity of training data, where faithfulness and diversity are two critical factors to effectiveness. However, promoting untargeted diversity can result in redundant samples with limited utility. To address these challenges, we propose a novel diffusion-based data augmentation approach, Sparse-Aware Semantic-Guided Diffusion Augmentation (SASG-DA). To enhance generation faithfulness, we introduce the Semantic Representation Guidance (SRG) mechanism by leveraging fine-grained, task-aware semantic representations as generation conditions. To enable flexible and diverse sample generation, we propose a Gaussian Modeling Semantic Modeling (GMSS) strategy, which models the semantic representation distribution and allows stochastic sampling to produce both faithful and diverse samples. To enhance targeted diversity, we further introduce a Sparse-Aware Semantic Sampling strategy to explicitly explore underrepresented regions, improving distribution coverage and sample utility. Extensive experiments on benchmark sEMG datasets, Ninapro DB2, DB4, and DB7, demonstrate that SASG-DA significantly outperforms existing augmentation methods. Overall, our proposed data augmentation approach effectively mitigates overfitting and improves recognition performance and generalization by offering both faithful and diverse samples.

**Index Terms**—Data augmentation, diffusion generation, surface electromyography, gesture recognition

## I. INTRODUCTION

Gesture recognition serves as a fundamental technology for advancing human-machine interaction. Among various gesture recognition modalities, surface electromyography (sEMG)-based approaches have gained increasing attention due to their non-invasive nature, high temporal resolution, and ability to directly capture muscle activation signals associated with voluntary movement [1]. sEMG sensors can be

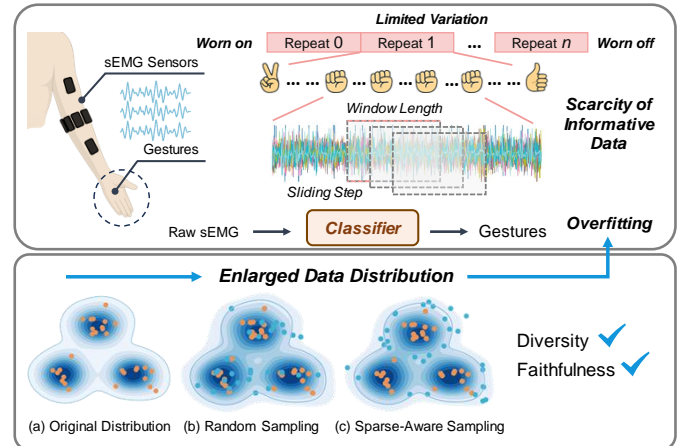


Fig. 1. Overfitting remains a persistent challenge in sEMG-based gesture recognition due to the scarcity of informative data. We alleviate this by generating faithful and diverse samples through diffusion-based augmentation. Our sparse-aware sampling strategy further encourages generation in underrepresented regions, effectively expanding the data distribution.

conveniently worn on the skin surface, making them well-suited for continuous and user-friendly deployment in real-world scenarios, particularly in fields such as rehabilitation training, prosthetic control [2], and wearable human-machine interfaces [3].

While deep learning has significantly improved gesture recognition performance, sEMG-based systems remain highly prone to overfitting due to the scarcity of informative training data. This scarcity arises from two main factors: the inherent difficulty in collecting large-scale sEMG datasets, and the prevalence of redundant information within the recorded data (Fig. 1). On the one hand, sEMG acquisition is labor-intensive and time-consuming, requiring substantial human and annotation costs, which constrain the overall dataset size. On the other hand, common collection protocols often involve subjects repeating each gesture multiple times within a single session. However, due to the limited variation across repetitions, the resulting data tend to be homogeneous. Moreover, sliding-window segmentation during preprocessing further introduces redundancy, as overlapping windows generate numerous similar samples. Therefore, increasing the size and diversity of available data is essential for improving the performance and generalization of sEMG-based gesture recognition systems.

Corresponding author: Dahong Qian.

Chen Liu, Can Han, Weishi Xu, and Dahong Qian are with the School of Biomedical Engineering, Shanghai Jiao Tong University, Shanghai 200240, China. (e-mail: lchen1206@sjtu.edu.cn).

Yaqi Wang is with the College of Media Engineering, Communication University of Zhejiang, Hangzhou, 310018, China.

Data augmentation offers a promising approach to increasing the size and diversity of training data. Previous studies on sEMG-based gesture recognition have explored both single-sample augmentation [4] and GAN-based augmentation [5], [6], which often suffer from limited diversity and unstable generation, respectively. More recently, diffusion-based augmentation has attracted significant interest for its ability to generate high-fidelity and diverse samples [7]. Nevertheless, despite its success in computer vision, only PatchEMG [8] has explored this direction in sEMG-based gesture recognition, focusing on generating high-quality data in a few-shot setting. In contrast, our work highlights two critical aspects of data augmentation: faithfulness and diversity [9]–[12]. Faithfulness ensures that generated samples remain consistent with the distribution of the original data, enabling the downstream model to learn from correct augmented data [10], while diversity enriches the original data distribution and helps the model learn robust and invariant features from diverse samples [9], [10]. For instance, DiffMix [9] and AGA [11] both emphasize introducing a diverse background while maintaining a faithful foreground, whereas DA-Fusion [12] considers diversity in the textual prompt space. However, direct application of these approaches to sEMG signals remains limited due to the lack of explicit textual prompts and a clear foreground-background structure. Furthermore, promoting untargeted diversity can result in redundant samples that offer limited incremental value, an aspect that only a few studies [13] have explored. Specifically, when diversity is introduced without considering the semantic coverage of the training set, the generated samples may cluster around already well-represented regions in the feature space, potentially reducing sample utility. Therefore, ensuring both faithfulness and targeted diversity helps expand the data distribution with informative samples, thereby improving the performance of sEMG-based gesture recognition systems (Fig. 1).

To this end, we propose a novel diffusion-based augmentation method, Sparse-Aware Semantic-Guided Diffusion Augmentation (SASG-DA) for sEMG-based gesture recognition, which aims to generate both faithful and diverse augmented samples. To enhance generation faithfulness, we introduce a Semantic Representation Guidance (SRG) mechanism, which leverages fine-grained, class-specific representations as semantic conditions to guide the diffusion training process. These semantic representations capture rich contextual information, enabling the model to generate synthetic samples that are not only realistic but also well-aligned with the target classes. To enable flexible and diverse sample generation, we further propose a Gaussian Modeling Semantic Sampling (GMSS) mechanism for the diffusion inference process, which introduces diversity by stochastically sampling novel semantic conditions for generation. However, untargeted diversity may lead to redundant samples. To this end, we propose a Sparse-Aware Semantic Sampling (SASS) mechanism that actively targets sparse regions in the semantic space for conditional sampling, which explicitly expands the coverage of the training distribution. In this setting, diversity arises not only from the inherent stochasticity of the diffusion process but also from the stochastic variation introduced in the semantic condition

space. Through the integrated strategy of Semantic Representation Guidance and Sparse-Aware Semantic Sampling, SASG-DA offers a principled augmentation method that enhances faithfulness and diversity, effectively mitigating overfitting and improving the performance and generalization of sEMG-based gesture recognition.

### Summary of Contributions

- 1) We propose a novel diffusion-based data augmentation method, Sparse-Aware Semantic-Guided Diffusion Augmentation (SASG-DA), for sEMG-based gesture recognition. The proposed method can provide both faithful and diverse augmented samples to mitigate the scarcity of informative training data.
- 2) To enhance generation faithfulness, we propose a Semantic Representation Guidance (SRG) mechanism which leverages fine-grained semantic representations as conditions, enabling the downstream model to learn from accurate and class-consistent information.
- 3) To enhance targeted generation diversity, we propose a Sparse-Aware Semantic Sampling (SASS) mechanism that actively focuses on underrepresented regions in the semantic space, explicitly expanding the training distribution and producing more informative, diverse augmented samples.
- 4) We comprehensively validate SASG-DA on three benchmark sEMG datasets, Ninapro DB2, DB4, and DB7, showing significant improvements over state-of-the-art methods and demonstrating the effectiveness of our augmentation approach in enhancing the performance and generalization.

## II. RELATED WORKS

### A. sEMG-based Gesture Recognition

Surface electromyography (sEMG) signals reflect muscle activation patterns and have been widely used for gesture recognition, especially in human–computer interaction and rehabilitation applications [1]. Recent advances in deep learning have significantly improved sEMG-based gesture recognition by enabling end-to-end learning from raw multi-channel signals. Numerous studies have focused on designing tailored network architectures, such as Spatio-Temporal Cross Networks (STCNet) [14], Kolmogorov-Arnold Network [15], and Transformer-based models [16], to enhance recognition accuracy. These models aim to capture the complex, non-stationary patterns in sEMG data and improve the performance and generalization of sEMG-based gesture recognition. In contrast, our work focuses on data augmentation as an orthogonal approach to enhance model performance and alleviate overfitting.

### B. Data Augmentation for sEMG-based Gesture Recognition

Data augmentation is crucial in improving generalization and mitigating overfitting, especially in scenarios with limited training data. Existing sEMG augmentation strategies can be broadly categorized into single-sample DA and generative-based DA.

Single-sample sEMG augmentation methods apply various transformations to individual data instances while preserving labels, typically in the time or frequency domain [17]. Prior work has systematically evaluated both traditional and novel data augmentation techniques for sEMG signals, such as magnitude warping and wavelet decomposition, demonstrating their effectiveness in improving classification accuracy [4]. Although single-sample DA methods are simple and computationally efficient, they often offer limited diversity and insufficient variations for enhancing model generalization [18].

Generative models provide a more principled approach to data augmentation by learning the underlying data distribution and synthesizing entirely new samples. Previous sEMG augmentation studies based on GANs [5], [6] and generative transformers (e.g., GPT) [19] have demonstrated their effectiveness in mitigating data scarcity and improving robustness to signal variability and noise. Building upon these advancements, diffusion-based models have recently emerged as a compelling alternative, offering superior generation ability in terms of both sample diversity and fidelity [7]. However, only a few studies have explored their application to sEMG-based gesture recognition. PatchEMG [8] is the first to apply diffusion models to few-shot sEMG signal synthesis, achieving high-fidelity augmentation and improved gesture recognition accuracy. Nevertheless, it primarily focuses on synthesizing high-quality data from a minimal number of samples, rather than exploring broader augmentation strategies or enhancing sample diversity.

To the best of our knowledge, PatchEMG [8] and our work are currently the only studies that leverage diffusion models for sEMG data augmentation. While PatchEMG focuses on the few-shot setting, our work explores a broader augmentation approach, aiming to mitigate the overfitting and improve the performance of sEMG-based gesture recognition.

### C. Diffusion Model Generation

Due to the various requirements of downstream tasks, diffusion models are designed with different generation objectives. Data augmentation, diverse generation, and minority sample generation are the most relevant to our work.

Recent diffusion-based data augmentation methods primarily aim to improve the faithfulness and diversity of generated samples [9]–[12]. For instance, DiffuseMix [20] preserves key semantics by concatenating generated and original samples using a binary mask. Other methods emphasize enhancing diversity of generated samples [9], [11], [12]. Among them, DiffMix [9] interpolates inter-class images during inference to increase diversity, producing novel counterfactual samples such as land birds in maritime settings; DA-Fusion boosts diversity by inserting and fine-tuning new tokens in the text encoder to capture novel visual concepts [12]. Beyond these efforts, only a few studies have explored the practical utility of augmented samples in downstream tasks [13], [21]. As untargeted diversity may lead to redundant or typical samples, GenDataAgent [21] incorporates downstream feedback to prioritize the generation of challenging samples. However, such feedback-driven approaches are often constrained by the slow

inference speed of diffusion models. Moreover, most diffusion-based image augmentation methods are not readily applicable to sEMG signals due to their modality-specific design.

A related but distinct objective is enhancing the diversity of diffusion generation, which has received comparatively less attention than improving generation quality [22]. Notable progress was made in CADs [22], where the authors showed that gradually annealing noise perturbations to conditional embeddings can significantly boost the diversity of generated samples. However, this approach is not intended for data augmentation.

Minority sample generation targets low-density regions of the data distribution, since diffusion model samplers inherently favor high-density regions of the data manifold [23]. Existing approaches typically address this limitation through gradient-based guidance, leveraging metrics such as the Hardness Score [23] or Minority Score [24]–[26] to generate minority samples. However, such gradient-guided methods often rely on additional external components and incur substantial computational overhead [25].

Distinct from prior works that focus solely on diverse or minority sample generation, our approach simultaneously emphasizes the faithfulness and diversity of generated data, which is crucial for effective data augmentation. Furthermore, our approach incorporates the Sparse-Aware Semantic Sampling (SASS) mechanism that explicitly expands the original data distribution to enhance augmentation utility, rather than focusing solely on rare samples in the target scenario. The latter approaches may generate data that deviates from the true distribution, which limits their usefulness for generalizable augmentation. Moreover, our SASS mechanism is designed to be computationally efficient.

## III. PRELIMINARY

### A. Diffusion Models for Data Generation

Denosing Diffusion Probabilistic Models (DDPMs) approximate complex data distributions by modeling a Markovian forward diffusion process and learning its corresponding reverse denoising process [27]. In this work, we adapt the DDPM for sEMG-based gesture recognition, aiming to mitigate overfitting through data augmentation.

The forward process transforms the original data distribution into a standard Gaussian by gradually adding noise. Formally, given an sEMG sample  $x_0 \in \mathbb{R}^{C \times L}$ , which represents a signal with  $C$  channels and  $L$  time steps, the noisy sequence  $\{x_t\}_{t=1}^T$  is generated by  $q(x_t|x_{t-1}) = \mathcal{N}(x_t; \sqrt{1 - \beta_t}x_{t-1}, \beta_t\mathbf{I})$ , where  $\beta_t$  denotes the noise schedule at timestep  $t$ .

The reverse process is a learned Markov chain that progressively denoises a sample from pure Gaussian noise to recover data resembling the original distribution. It is defined by  $p_\theta(x_{t-1}|x_t) = \mathcal{N}(x_{t-1}; \mu_\theta(x_t, t), \Sigma_\theta(x_t, t))$ , where  $\mu_\theta$  and  $\Sigma_\theta$  are parameterized by a neural network  $\theta$  [27].

Although the reverse process generates samples using the predicted means  $\mu_\theta$ , it is common in practice to express  $\mu_\theta(x_t, t)$  in terms of either the predicted clean data  $\hat{x}_0(x_t, t; \theta)$  or the predicted noise  $\hat{\epsilon}(x_t, t; \theta)$ . Following the Diffusion-TS approach [28], our model is trained to predict an estimate  $\hat{x}_0$

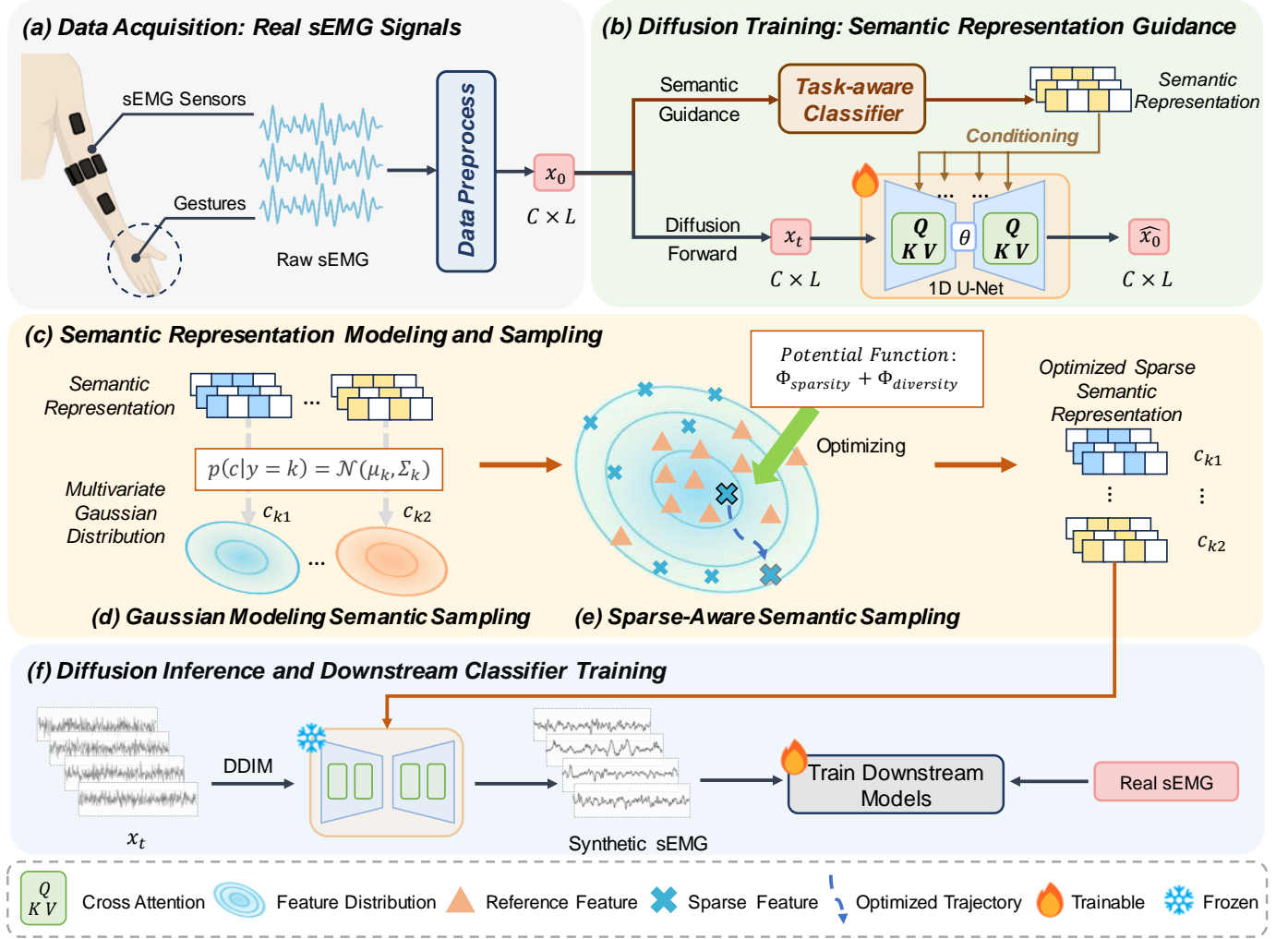


Fig. 2. Overview of the proposed SASG-DA approach based on diffusion model. (b) SASG-DA enhances generation faithfulness by introducing semantic representations to guide diffusion training. (c) During inference, by (d) modeling semantic representation distribution, SASG-DA performs (e) Sparse-Aware Semantic Sampling to target the sparse regions in the semantic space and expand the data distribution. (f) The optimized sparse semantic representation are then used as condition inputs for diffusion reverse and generate synthetic sEMG signals for downstream model training.

directly. This leads to a simplified training objective known as denoising score matching, formulated as:

$$\mathcal{L}_{\text{simple}} = \mathbb{E}_{x_0, x_t} [\|x_0 - \hat{x}_0(x_t, t; \theta)\|^2], \quad (1)$$

where  $x_t = \sqrt{\bar{\alpha}_t}x_0 + \sqrt{1 - \bar{\alpha}_t}\epsilon$ ,  $\epsilon \sim \mathcal{N}(0, \mathbf{I})$ , and  $\bar{\alpha}_t$  is related to the noise schedule at timestep  $t$ .

To further improve signal generative fidelity, we incorporate the same Fourier-based loss employed in Diffusion-TS [28]:

$$\mathcal{L}_{\text{Fourier}} = \mathbb{E}_{x_0, x_t} [\|\mathcal{FFT}(x_0) - \mathcal{FFT}(\hat{x}_0(x_t, t; \theta))\|^2]. \quad (2)$$

To generate data that aligns with specific class semantics, class-conditional diffusion models incorporate label information throughout the denoising process. In our case, the simplified training objective becomes:

$$\mathcal{L}_{\text{cond}} = \mathbb{E}_{x_0, x_t, y} [\|x_0 - \hat{x}_0(x_t, t, y; \theta)\|^2], \quad (3)$$

where  $y$  is the class label.

Once trained, the model can generate new samples by drawing  $x_t \sim \mathcal{N}(0, \mathbf{I})$  and iteratively applying the reverse transitions.

## IV. METHODOLOGY

### A. Overview

To mitigate the overfitting issue commonly encountered in sEMG-based gesture recognition, we propose a novel augmentation method, SASG-DA, based on diffusion models by offering faithful and diverse samples. To enhance generation faithfulness, SASG-DA conditions the diffusion model on fine-grained semantic representations extracted from the training data, ensuring that generated samples are both realistic and class-consistent. To enable flexible and diverse generation, we propose a Gaussian Modeling Semantic Sampling (GMSS) mechanism that approximates the semantic representation distribution based on a Gaussian assumption. To further explicitly expand the coverage of the training distribution and enhance data utility, we design a Sparse-Aware Semantic Sampling (SASS) mechanism, which encourages sampling from sparse or underrepresented regions of the modeled semantic space. The overall framework is illustrated in Fig. 2. Given a target class, our method first samples a semantic representation via

SASS to guide the diffusion model in generating new gesture samples. These samples are then added to the training set to boost the performance of gesture recognition.

### B. Semantic Representation Guidance

Faithfulness is a key factor in data augmentation tasks. Specifically, it requires that synthetic samples preserve the distinctive features of their target classes, thereby ensuring that the downstream classifier learns from accurate and class-consistent information [10]. However, in conventional class-conditioned diffusion models, label conditions alone often provide only coarse-grained guidance, lacking sufficient semantic richness to generate highly faithful samples.

To overcome this limitation, we propose using fine-grained semantic representations as conditioning inputs. These continuous, class-specific features serve as informative guidance signals, allowing the model to generate more semantically aligned and realistic samples. Specifically, semantic representations  $f \in \mathcal{R}^{D_c}$  are extracted from a pretrained task-aware classifier and integrated into the diffusion process via cross-attention mechanisms. We further apply dropout to the semantic features during training to improve robustness and mitigate overfitting to the conditioning input. In addition, label information is retained and incorporated through additive conditioning. The overall training objective combining (2) and (3) is modified as follows:

$$\begin{aligned} \mathcal{L}_{SRG} = & \mathbb{E}_{x_0, x_t, t, y, f} \left[ \|x_0 - \hat{x}_0(x_t, t, y, f; \theta)\|^2 \right. \\ & \left. + \|\mathcal{F}\mathcal{F}\mathcal{T}(x_0) - \mathcal{F}\mathcal{F}\mathcal{T}(\hat{x}_0(x_t, t, y, f; \theta))\|^2 \right] \end{aligned} \quad (4)$$

### C. Gaussian Modeling Semantic Sampling

In class-conditioned diffusion frameworks, the quality and diversity of the generated samples depend heavily on the design of the conditioning signal. To enable flexible and diverse generation, we propose a simple yet effective Gaussian Modeling Semantic Sampling (GMSS) mechanism. Specifically, we approximate the semantic representation distribution of each class as a multivariate Gaussian, a widely adopted approach in representation learning, which facilitates diverse sampling while maintaining semantic consistency.

Given a labeled training set, we extract semantic representations for all samples using a pretrained task-aware encoder  $E(\cdot)$ , such as a backbone CNN or transformer trained on the sEMG-based gesture classification task. For each class  $k$ , we construct its semantic feature set  $\mathcal{F}_k = \{f_i = E(x_i) \mid y_i = k\}$  and estimate its empirical mean and covariance:

$$\mu_k = \frac{1}{|\mathcal{F}_k|} \sum_{f \in \mathcal{F}_k} f, \quad \Sigma_k = \frac{1}{|\mathcal{F}_k| - 1} \sum_{f \in \mathcal{F}_k} (f - \mu_k)(f - \mu_k)^\top. \quad (5)$$

We then model the semantic representation distribution as a multivariate Gaussian  $\mathcal{N}(\mu_k, \Sigma_k)$ . During diffusion inference, a new semantic representation  $\tilde{f}_k$  can be sampled as:

$$\tilde{f}_k \sim \mathcal{N}(\mu_k, \Sigma_k). \quad (6)$$

The sampled feature  $\tilde{f}_k$  serves as a continuous condition to guide the reverse process of the diffusion model, enabling the generation of semantically aligned yet diverse gesture samples within class  $k$ .

Compared to label-based conditioning, which restricts generation to discrete and often coarse class labels, GMSS provides a continuous, distribution-based conditioning space that enables infinite and controllable sampling within each class. By sampling from different regions of the semantic representation distribution, GMSS allows the diffusion model to cover regions beyond the original training set while preserving semantic faithfulness. This not only increases intra-class diversity but also expands the effective data manifold, thereby improving the generalization performance of classifiers. In this way, diversity arises not only from the inherent stochasticity of the diffusion process but also from the stochastic variation introduced in the semantic condition space.

### D. Sparse-Aware Semantic Sampling

While GMSS allows class-consistent sampling in a continuous semantic representation space, the diffusion model inherently tends to generate samples in dense regions of the feature distribution, thereby failing to explore underrepresented or sparsely populated areas [23]. To address this limitation, we propose a Sparse-Aware Semantic Sampling (SASS) strategy that explicitly guides the generation process toward sparse regions in the data distribution. SASS employs a global-local sampling strategy: at the global level, we identify candidate features that are likely to lie in sparse regions of the distribution; at the local level, we optimize these candidates using a potential function that jointly encourages sparsity and diversity.

Specifically, we first generate an oversampled set of features  $\tilde{f}$  from the class-specific Gaussian distribution  $\mathcal{N}(\mu_k, \Sigma_k)$ , denoted as the candidate set  $C_k$ . This random oversampling retains class consistency while providing a broad coverage of the semantic representation space.

To systematically identify potential sparse candidates within the oversampled pools, we adopt a *rarity score* metric proposed by [29]. Specifically, we define the original training samples of each class as the reference set  $R_k$  and establish  $k$ -NN spheres in the reference set, where each sphere is centered at a reference sample and its neighbors are also reference samples. For each candidate sample, the *rarity score* is computed as the radius of the smallest  $k$ -NN sphere that contains it. Intuitively, candidates located in denser regions will fall into smaller-radius spheres, while those closer to sparse regions will yield higher *rarity scores*. In addition, the *rarity scores* of outliers are set to zero. By ranking all candidates according to their *rarity scores*, we select high-rarity candidates as a preliminary pool of potential sparse conditions  $\check{C}_k$ .

Although the *rarity score* enables global selection of sparse candidates, further optimization is needed to enhance local sparsity and inter-sample diversity. Inspired by physical potential fields, we model candidate samples as repulsive particles in the feature space and define a density-driven potential

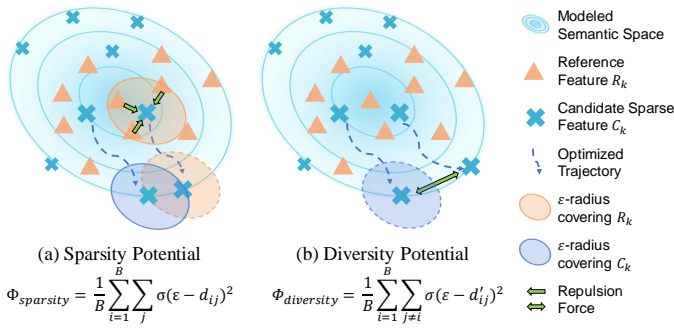


Fig. 3. Sparse-Aware Semantic Sampling. Candidate sparse features (blue) are optimized in the modeled semantic space using two potential functions. (a) The sparsity potential applies a repulsive force between candidate and reference features (orange), pushing candidates toward sparse regions. (b) The diversity potential encourages mutual repulsion among candidates to spread out within the semantic space.

function that quantifies local feature crowding. Specifically, each candidate is guided to reside in a low-potential (i.e., sparsely populated) region by explicitly minimizing a smooth neighborhood density measure.

Formally, for each selected candidate feature  $\tilde{f}$ , we define its local neighborhood as the set of reference samples within an  $\epsilon$ -radius in the semantic space. In this way, each neighborhood is centered on the candidate feature, while its neighbors are reference samples from the same class. To make this neighborhood count differentiable to gradient-based optimization, we replace the hard count with a smooth approximation using a sigmoid function  $\sigma$ :

$$N_i = \sum_j \sigma(\epsilon - d_{ij}), \quad (7)$$

where  $\epsilon$  defines the effective neighborhood radius, and

$$d_{ij} = \|\tilde{f}_i - f_j\|, \tilde{f}_i \in \tilde{C}_k, f_j \in R_k. \quad (8)$$

We then formulate a sparsity potential function that penalizes high local density:

$$\Phi_{sparsity} = \frac{1}{B} \sum_{i=1}^B N_i^2. \quad (9)$$

By minimizing this potential through gradient-based updates to the candidate feature  $\tilde{f}$ , the optimized features are adaptively repelled from high-density clusters and pushed into sparse regions of the class manifold.

Meanwhile, to further ensure that the generated candidates themselves remain sufficiently diverse and do not collapse into redundant clusters, we introduce an additional repulsion mechanism among the candidate samples. Similarly, we enforce pairwise separation between candidate features by defining a diversity potential:

$$\Phi_{diversity} = \frac{1}{B} \sum_{i=1}^B \sum_{j \neq i} \sigma(\epsilon - d'_{ij})^2, \quad (10)$$

where

$$d'_{ij} = \|\tilde{f}_i - \tilde{f}_j\|, \tilde{f}_i, \tilde{f}_j \in \tilde{C}_k. \quad (11)$$

Minimizing  $\Phi_{diversity}$  encourages candidate samples to spread apart within the feature space, discouraging trivial duplication and enforcing local sample-level diversity.

### Algorithm 1 Sparse-aware Semantic Sampling

**Require:** Reference set  $R_k$ , Gaussian Modeling semantic representation distribution  $\mathcal{N}(\mu_k, \Sigma_k)$ , neighborhood radius  $\epsilon$ , iterations  $iter$ , learning rate  $\eta$ .

**Ensure:** Optimized sparse and diverse semantic representation set  $S_k$ .

- 1: Generate candidate set  $C_k$  by sampling  $10 \times B$  features from  $\mathcal{N}(\mu_k, \Sigma_k)$ .
- 2: Compute *rarity score* for each  $\tilde{f}_i$  in  $C_k$ .
- 3: Rank  $\tilde{f}_i$  by *rarity score* descending, select top  $B$  to form  $\tilde{C}_k$ .
- 4: **for** iteration  $t = 1$  to  $iter$  **do**
- 5:   Compute sparsity potential  $\Phi_{sparsity}$  by (9).
- 6:   Compute diversity potential  $\Phi_{diversity}$  by (10).
- 7:   Combine total objective:  $\Phi = \Phi_{sparsity} + \Phi_{diversity}$ .
- 8:   Compute gradient:  $\nabla_{\tilde{C}_k} \Phi$ .
- 9:   Update:  $\tilde{C}_k \leftarrow \tilde{C}_k - \eta \cdot \nabla_{\tilde{C}_k} \Phi$ .
- 10: **end for**
- 11: Evaluate classifier confidence for each  $\tilde{f}_i$  in  $\tilde{C}_k$ ; keep only those above threshold.
- 12: Supplement with high-fidelity  $\tilde{f}_i \sim \mathcal{N}(\mu_k, 0.5\Sigma_k)$ .
- 13: **return**  $S_k$ .

The final objective thus combines density-based repulsion from training samples and mutual repulsion among candidates, yielding a balanced potential field:

$$\Phi = \Phi_{sparsity} + \Phi_{diversity}. \quad (12)$$

This dual-potential approach provides targeted control over how generated samples align with underrepresented regions and maintain sufficient pairwise separation, resulting in optimized features that are both sparse and diverse.

Before feeding the optimized sparse features into the diffusion model as conditional guidance, we further ensure the quality of these conditions through a confidence-based filtering step. Specifically, we evaluate each optimized feature's confidence score using the task-aware classifier and retain only those exceeding a predefined lower threshold. To compensate for discarded low-confidence samples and maintain balanced class coverage, the semantic representation conditions are further supplemented with high-fidelity samples drawn from GMSS, parameterized by the distribution  $\mathcal{N}(\mu_k, 0.5\Sigma_k)$ . This ensures that the final condition set combines sparsity, diversity, and discriminative reliability for more effective diffusion-based augmentation. The overall algorithm is shown in Algorithm 1. To ensure efficiency and consistency, all condition features are synthesized offline, organized by class, before initiating the reverse diffusion process.

## V. EXPERIMENTS AND RESULTS

### A. Datasets

To evaluate the effectiveness of the proposed approach, we conduct data augmentation experiments on three public sEMG benchmark datasets, namely Ninapro DB2 [30], DB4 [31], and DB7 [32], as summarized in Table I. These datasets encompass a diverse range of gesture classes and subjects, providing

TABLE I  
CHARACTERISTICS AND SETUP OF THREE PUBLIC SEMG DATASETS.

Dataset	Ninapro DB2	Ninapro DB4	NinaproDB7
Subjects	40	10	20
Channels	12	12	12
Sampling rate	2000Hz	2000Hz	2000Hz
Trials	6	6	6
Training Trials	1,3,4,6	1,3,4,6	1,3,4,6
Testing Trials	2,5	2,5	2,5
Gestures	49	52	40

a comprehensive testbed for evaluating generalization. Each dataset contains multi-channel sEMG signals acquired using sparse-density acquisition systems with a sampling rate of 2 kHz. During preprocessing, the raw sEMG signals of each subject are segmented via a sliding window of length 200 ms with a step size of 40 ms, and then standardized channel-wise. To ensure consistency with previous studies [15], [16] and focus on gesture-related categories, the rest class is excluded during preprocessing. Following established protocols [15], [16] for gesture recognition based on sEMG, we adopt a cross-trial paradigm in which the training and testing sets are divided based on the trial information, as mentioned in Table I.

### B. Evaluation Metrics

To comprehensively evaluate the effectiveness of our proposed SASG-DA approach for sEMG-based gesture recognition, we employ the following three categories of metrics: classification performance under the intra-subject paradigm, generation quality metrics, and sparsity evaluation metrics. All latent features involved in evaluation are extracted by a pretrained classifier.

We evaluate the classification performance under the intra-subject setting, where each subject is trained and tested separately. Accuracy (ACC) is reported as the average classification accuracy across all subjects and serves as the primary indicator of the model’s classification ability. In addition, the average precision (Pre), recall (Rec), and F1-score are calculated across all subjects to offer a more detailed assessment of the model’s classification performance.

To assess the quality of samples generated by the diffusion model, we adopt the Fréchet Inception Distance (FID) [33] and Category Accuracy Score (CAS). FID quantifies the distributional similarity between real and generated samples in a latent feature space. CAS evaluates the semantic consistency of generated samples by measuring the classification accuracy of generated data using a classifier trained solely on real samples. It reflects the model’s ability to generate the intended target classes.

To further analyze the diversity and sparsity of generated samples, we employ three sparsity-aware metrics derived from [23], [25], following the same evaluation settings: (1) Average KNN Distance (AvgKNN) measures the average distance from a sample to its nearest neighbors in the feature space ( $k = 5$ ). (2) Local Outlier Factor (LOF) [34] assesses how the local density of a sample deviates from that of its neighbors ( $k = 20$ ). (3) Rarity Score [29] explicitly quantifies the rarity of individual generated samples ( $k = 5$ ). We

compare the sparsity of generated samples against that of real samples.

### C. Baseline Models

To evaluate the data augmentation performance of our proposed approach, we adopt three backbone models: Crossformer, TDCT, and STCNet.

Crossformer [35] is a popular Transformer-based model for time series forecasting, which has also demonstrated superior performance in sEMG classification tasks due to its ability to effectively model cross-time and cross-channel dependencies and extract multi-scale temporal features. In our experiments, we set the segment length to 16, the window size to 2, and the number of layers to 5.

TDCT [16] is a Transformer-based model tailored for sEMG-based gesture recognition. It incorporates temporal depthwise convolution into the self-attention mechanism to enhance sequence modeling while reducing parameters and computational cost. We follow the original architecture and settings from [16].

STCNet [14] is also specifically developed for sEMG-based gesture recognition. It combines convolutional and recurrent layers with a spatio-temporal block to enhance feature extraction across time and space. It also incorporates a rolling convolution module to capture the spatial structure inherent in the placement of the sEMG sensor. The input is reshaped to  $(C, 20, 20)$  following [14], and other configurations remain unchanged.

### D. Experimental Settings

The experiments are divided into two parts: Diffusion-based data augmentation and downstream classification. The diffusion model is implemented based on a 1D U-Net and is trained exclusively on the original training set. It employs 1000 diffusion steps with a cosine noise schedule and is optimized using the  $x_0$ -prediction objective with the Adam optimizer (learning rate:  $1e-5$ , batch size: 128) for 20,000 iterations. A conditional dropout rate of 0.05 is applied during training to enhance generalization. During sampling, we use DDIM with 500 steps to generate synthetic samples. All pretrained classifiers used during the generation process are implemented using Crossformer and are trained solely on the original training set. For sparse-aware sampling, the hyperparameters involved are empirically set to 200 iterations (*iter*), a neighborhood radius ( $\epsilon$ ) of 3.0, and a learning rate ( $\eta$ ) of 10.0 during optimization. The confidence threshold for filtering sparse samples is set to 0.15.

Following the settings in [9], we randomly shuffle the original training data and the generated samples during the experiments. The resulting augmented dataset, which is twice the size of the original training set, is then used for downstream classification. We evaluate the performance using three different backbone classifiers. During training, we employ the SGD optimizer with an initial learning rate of 0.01, which is reduced by a factor of 0.1 at the 60th epoch. The batch size is set to 256, and all models are trained for 100 epochs. All results are reported as the mean over three runs with different random seeds.

TABLE II

PERFORMANCE COMPARISON WITH SOTAs IN TERMS OF ACC (%), PRE(%), REC(%), AND F1(%) ON DATASET DB7 USING THREE DIFFERENT BACKBONES. RESULTS ARE AVERAGED AMONG THREE RANDOMIZED SPLITS. BEST PERFORMANCES ARE HIGHLIGHTED IN BOLD.

Aug. Method	Crossformer				TDCT				STCNet			
	Acc	Pre	Rec	F1	Acc	Pre	Rec	F1	Acc	Pre	Rec	F1
Baseline	77.97	78.86	78.37	78.61	73.54	74.99	73.96	74.46	73.61	75.10	74.17	74.63
Jittering & Scaling	78.05	79.12	78.44	78.78	74.10	75.44	74.53	74.92	72.28	73.98	72.88	73.43
Upsample	<u>80.71</u>	<u>81.42</u>	<u>81.17</u>	<u>81.29</u>	74.67	75.95	75.00	75.47	79.92	<u>81.64</u>	80.50	81.07
FreqMask	77.99	79.02	78.62	78.82	75.59	77.11	76.10	76.60	78.87	80.06	79.47	79.76
RIM	79.04	79.75	79.49	79.62	76.12	77.28	76.55	76.91	76.93	78.18	77.48	77.83
Dominant Shuffle	79.41	80.22	79.80	80.01	75.21	77.03	75.67	76.34	78.92	80.37	79.46	79.91
Mixup	76.99	77.79	77.58	77.68	75.17	76.03	75.68	75.85	73.90	75.18	74.55	74.86
STAug	77.43	78.30	77.95	78.12	75.32	76.29	75.72	76.00	73.53	74.77	74.22	74.49
FreqMix	79.79	80.96	80.22	80.59	76.24	<u>77.68</u>	76.56	<u>77.12</u>	78.35	79.94	78.86	79.40
SimPSI	78.23	78.94	78.60	78.77	74.12	75.43	74.52	74.97	74.51	75.92	75.16	75.54
DiffMix	78.14	78.90	78.52	78.71	74.44	75.40	74.86	75.13	74.26	75.51	74.89	75.20
Minority	79.86	80.30	80.37	80.33	75.14	75.86	75.67	75.76	79.84	80.53	80.37	80.45
CADS	80.41	80.83	80.86	80.84	<u>76.36</u>	77.16	<u>76.75</u>	76.95	<u>80.55</u>	81.28	<u>81.07</u>	<u>81.17</u>
SASG-DA (Ours)	<b>81.31</b>	<b>81.89</b>	<b>81.75</b>	<b>81.82</b>	<b>78.77</b>	<b>79.73</b>	<b>79.23</b>	<b>79.48</b>	<b>82.15</b>	<b>83.07</b>	<b>82.68</b>	<b>82.87</b>

TABLE III

PERFORMANCE COMPARISON WITH SOTAs IN TERMS OF ACC (%), PRE(%), REC(%), AND F1(%) ON DATASET DB4 USING THREE DIFFERENT BACKBONES. RESULTS ARE AVERAGED AMONG THREE RANDOMIZED SPLITS. BEST PERFORMANCES ARE HIGHLIGHTED IN BOLD.

Aug. Method	Crossformer				TDCT				STCNet			
	Acc	Pre	Rec	F1	Acc	Pre	Rec	F1	Acc	Pre	Rec	F1
Baseline	65.78	66.97	67.49	67.23	62.62	64.18	64.34	64.26	61.25	63.43	63.05	63.24
Jittering & Scaling	66.01	67.35	67.80	67.57	63.05	64.60	64.75	64.67	59.97	62.23	61.74	61.98
Upsample	67.62	69.23	69.29	69.26	63.37	65.16	65.23	65.19	<u>68.44</u>	<u>70.40</u>	<u>70.14</u>	<u>70.27</u>
FreqMask	66.67	68.08	68.35	68.21	64.50	66.31	66.23	66.27	67.08	68.99	68.82	68.90
RIM	67.18	68.31	68.90	68.60	64.47	65.75	66.21	65.98	65.08	66.58	66.77	66.67
Dominant Shuffle	67.21	68.41	68.96	68.68	64.22	66.01	66.06	66.03	65.89	67.89	67.69	67.79
Mixup	66.21	67.48	67.86	67.67	64.50	65.96	66.20	66.08	62.13	63.95	63.82	63.88
STAug	66.41	67.77	68.09	67.93	63.96	65.31	65.67	65.49	61.46	63.36	63.10	63.23
FreqMix	68.51	<u>70.03</u>	70.25	70.14	65.45	<u>67.08</u>	67.15	67.11	66.69	68.73	68.38	68.55
SimPSI	66.72	67.93	68.40	68.16	64.06	65.54	65.78	65.66	62.44	64.48	64.06	64.27
DiffMix	66.08	67.21	67.81	67.51	62.14	63.35	63.83	63.59	63.22	64.89	64.99	64.94
Minority	68.39	69.49	70.03	69.76	64.47	65.86	66.13	65.99	66.74	68.38	68.42	66.40
CADS	<u>68.91</u>	69.99	<u>70.57</u>	<u>70.28</u>	<u>65.58</u>	67.03	<u>67.33</u>	<u>67.18</u>	67.45	68.84	69.13	68.98
SASG-DA (Ours)	<b>69.73</b>	<b>70.73</b>	<b>71.38</b>	<b>71.05</b>	<b>67.74</b>	<b>69.02</b>	<b>69.42</b>	<b>69.22</b>	<b>70.05</b>	<b>71.37</b>	<b>71.75</b>	<b>71.56</b>

TABLE IV

PERFORMANCE COMPARISON WITH SOTAs IN TERMS OF ACC (%), PRE(%), REC(%), AND F1(%) ON DATASET DB2 USING THREE DIFFERENT BACKBONES. RESULTS ARE AVERAGED AMONG THREE RANDOMIZED SPLITS. BEST PERFORMANCES ARE HIGHLIGHTED IN BOLD.

Aug. Method	Crossformer				TDCT				STCNet			
	Acc	Pre	Rec	F1	Acc	Pre	Rec	F1	Acc	Pre	Rec	F1
Baseline	74.63	75.89	75.44	75.66	70.00	71.44	70.83	71.13	69.71	71.86	70.83	71.34
Jittering & Scaling	74.36	75.75	75.20	75.47	70.08	71.67	70.94	71.30	68.46	70.78	69.61	70.19
Upsample	75.84	77.18	76.85	77.01	70.05	71.66	70.91	71.28	<u>74.38</u>	<u>76.69</u>	<u>75.36</u>	<u>76.02</u>
FreqMask	74.37	75.90	75.36	75.63	71.22	72.90	72.16	72.53	73.86	75.70	74.89	75.29
RIM	75.69	76.81	76.53	76.67	71.36	72.72	72.28	72.50	72.14	73.78	73.20	73.49
Dominant Shuffle	75.82	77.10	76.63	76.86	71.02	73.01	71.91	72.46	74.38	76.17	75.33	75.75
Mixup	74.45	75.65	75.45	75.55	71.13	72.47	72.12	72.29	69.46	71.44	70.58	71.01
STAug	74.49	75.65	75.40	75.52	71.02	72.36	71.94	72.15	69.52	71.45	70.72	71.08
FreqMix	<u>77.07</u>	<u>78.57</u>	77.86	<u>78.21</u>	71.47	<u>73.56</u>	72.33	72.94	73.92	75.97	74.94	75.45
SimPSI	74.58	75.74	75.42	75.58	70.52	71.98	71.43	71.70	70.91	72.80	72.00	72.40
DiffMix	74.84	76.07	75.74	75.90	69.47	70.86	70.49	70.67	70.33	72.01	71.49	71.75
Minority	76.89	77.59	77.78	77.68	71.31	72.34	72.16	72.25	73.48	74.57	74.52	74.54
CADS	77.03	77.74	<u>77.87</u>	77.80	<u>72.33</u>	73.27	<u>73.08</u>	<u>73.17</u>	74.33	75.34	75.29	75.31
SASG-DA (Ours)	<b>77.86</b>	<b>78.82</b>	<b>78.73</b>	<b>78.77</b>	<b>74.31</b>	<b>75.46</b>	<b>75.20</b>	<b>75.33</b>	<b>76.36</b>	<b>77.59</b>	<b>77.29</b>	<b>77.44</b>

TABLE V  
ABLATIONS OF EACH MODULE IN TERMS OF ACC (%) ON DB7 AND DB4. BEST PERFORMANCES ARE HIGHLIGHTED IN BOLD.

Augmentation	Label condition	GMSS	SASS	DB7			DB4		
				Crossformer	TDCT	STCNet	Crossformer	TDCT	STCNet
×	×	×	×	77.97	73.54	73.61	65.78	62.62	61.25
✓	✓	×	×	80.49	77.09	80.62	68.81	66.04	68.19
✓	✓	✓	×	80.87	77.57	81.67	69.44	66.99	69.41
✓	✓	×	✓	<b>81.31</b>	<b>78.77</b>	<b>82.15</b>	<b>69.73</b>	<b>67.74</b>	<b>70.05</b>

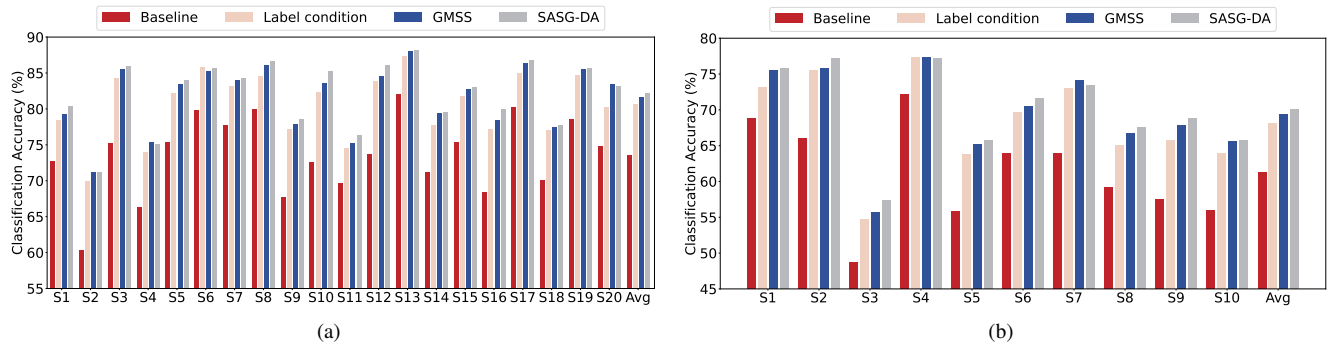


Fig. 4. Classification accuracy (%) ablation results for all the subjects from (a) DB7 and (b) DB4.

### E. Comparison with the State-of-the-arts

We compare our method against a comprehensive set of state-of-the-art data augmentation approaches. Specifically, we evaluate five single-sample DA methods tailored for time series: Jittering & Scaling [36], Upsample [37], FreqMask [38], RIM [39], and Dominant Shuffle [17]. We also consider four mix-based DA methods: Mixup [40], STAug [41], FreqMix [38], and SimPSI [42]. In addition, three diffusion-based DA methods are included. DiffMix [9] is a simple yet effective generative data augmentation strategy that leverages inter-class image interpolation to produce both faithful and diverse samples. Minority [25] leverages gradient guidance to synthesize samples in low-density regions. CADs [22] enhances sample diversity by injecting stochastic perturbations into conditional inputs during the inference process. For single-sample and mix-based DA methods, we adopt a batch-wise augmentation strategy, whereas for diffusion-based methods and RIM, we jointly train the original and augmented samples to preserve data distribution better and improve model generalization. For fairness, all SOTA methods are reproduced using official code when available, or reimplemented based on recommended or optimal settings.

The results in Table II, Table III, and Table IV demonstrate that our method consistently outperforms the state-of-the-art (SOTA) on three datasets and with all three backbones, which confirms its generalizability and consistent effectiveness when used as a data augmentation method. Compared to the next best method, CADs [22], which enhances diversity in diffusion-based augmentation, our method achieves an average accuracy gain of **1.7%** across all datasets and backbones. This confirms the effectiveness of guiding sample generation toward sparse regions, resulting in more informative and complementary samples for data augmentation. Compared to Minority [25], our approach achieves better performance by

not only improving diversity but also enhancing the faithfulness of generated samples, i.e., their alignment with class-consistent semantics. This improvement in sample fidelity allows the augmented data to better support classifier learning, leading to more substantial gains in accuracy.

### F. Ablation Study

1) *Module Ablation*: To evaluate the contribution of each component in our proposed approach, we conduct a series of ablation experiments by progressively integrating each module. The results are shown in Table V. We first conduct ablation experiments using two baselines: training without any data augmentation and using a simple label-conditioned generation. The results show that data augmentation effectively alleviates the limitations of the training set and improves the performance of gesture recognition. Subsequently, we introduce semantic representations as conditions and adopt the GMSS strategy, which yields significant improvements across all backbones and datasets, demonstrating that the semantic guidance and sampling enhances the faithfulness and diversity of the generated samples. Finally, we incorporate the SASS strategy to explicitly expand the distribution of the training data, which further improves the downstream classification performance. Compared to the baseline, our method achieves an average improvement of **5.8%**, confirming its effectiveness and generalizability.

2) *Inter-Subject Variability Ablation*: It is well known that sEMG signals exhibit significant subject-level variability due to factors such as muscle anatomy, skin-electrode impedance, and electrode placement. Fig. 4 illustrates the classification accuracy for each subject from the DB7 and DB4 datasets. Our method yields consistent improvements for the majority of subjects, demonstrating its effectiveness in enhancing general performance.

TABLE VI  
HYPERPARAMETERS ABLATIONS ON DB7 AND DB4 UNDER DIFFERENT SETTINGS FOR THREE BACKBONES.

<i>iter</i>	$\epsilon$	threshold	DB7					DB4				
			FID	CAS	Crossformer	TDCT	STCNet	FID	CAS	Crossformer	TDCT	STCNet
200	2.0	0.15	1.32	61.08	81.07	78.51	81.82	1.39	57.46	69.51	67.84	69.98
200	2.5	0.15	1.33	59.99	81.13	78.80	82.16	1.41	56.70	69.64	67.95	70.15
200	3.0	0.15	1.35	58.65	81.31	78.77	82.15	1.42	56.28	69.73	67.74	70.05
100	3.0	0.15	1.32	59.83	80.99	78.92	82.02	1.40	57.14	69.65	67.61	70.04
200	3.0	0.15	1.35	58.65	81.31	78.77	82.15	1.42	56.28	69.73	67.74	70.05
300	3.0	0.15	1.37	57.62	81.24	78.83	82.18	1.43	55.65	69.59	67.78	70.08
200	3.0	0.05	-	-	81.00	78.63	81.93	-	-	69.72	67.59	69.86
200	3.0	0.15	-	-	81.31	78.77	82.15	-	-	69.73	67.74	70.05
200	3.0	0.25	-	-	80.97	78.55	81.86	-	-	69.63	67.58	69.98

3) *Hyperparameters Ablation*: To better understand the influence of key hyperparameters on the performance of our approach, we conduct ablation studies focusing on three key hyperparameters: the number of iterations (*iter*) during sparse-aware sampling, the neighborhood radius ( $\epsilon$ ), and the confidence threshold for filtering sparse samples. The first two parameters control the degree of sparsity during sample generation: larger iterations and larger neighborhood radii produce samples with greater sparsity (e.g., higher FID and lower CAS). The confidence threshold serves as a filter mechanism to avoid introducing low-quality samples. The experimental ablations in Table VI present the results across different settings on DB7 and DB4 using multiple backbone classifiers. We observe that increasing *iter* and  $\epsilon$  slightly affects classification accuracy, suggesting that our sparse-aware sampling strategy is relatively stable under varying sparsity levels. Additionally, performance remains consistent across a range of confidence thresholds, indicating that the filtering mechanism does not overly restrict sample diversity. Overall, these results highlight the robustness of our method concerning key hyperparameter choices and confirm that it generalizes well without requiring sensitive tuning.

## VI. FURTHER ANALYSIS AND DISCUSSION

### A. The Faithfulness of Generated Samples

To further validate the faithfulness of generated samples, we conduct quantitative evaluations of generation metrics, distributional analyses, and qualitative sample visualizations. As shown in Table VII, both the Fréchet Inception Distance (FID) and Category Accuracy Score (CAS) consistently demonstrate the effectiveness of the proposed Semantic Representation Guidance mechanism in guiding the generation process. Specifically, the lower FID values indicate that the generated samples are closer to the real data distribution,

TABLE VII  
QUANTITATIVE EVALUATIONS OF GENERATION QUALITY ON DB7 AND DB4.

Guidance	DB7		DB4	
	FID	CAS	FID	CAS
Label Condition	2.77	49.83	2.95	45.99
GMSS	0.88	71.73	0.87	68.09

while higher CAS values reflect improved alignment with class-specific characteristics. These results suggest that incorporating fine-grained semantic representations as conditional information allows the model to synthesize more realistic and discriminative samples for each class.

To verify the distributional faithfulness of the generated samples, we randomly select a subject from DB7, DB4, and DB2 for analysis. For each subject, features are extracted from both real and generated samples using a pretrained classifier, and subsequently projected into a two-dimensional space via t-SNE. As shown in Fig. 5, the generated samples consistently align with the corresponding real samples in the embedding space, demonstrating a high degree of distributional similarity. These results indicate that the proposed Semantic Representation Guidance mechanism effectively preserves the intrinsic structure of the original data, facilitating the generation of class-consistent samples within the real data manifold.

We further provide qualitative comparisons by randomly selecting one sample from each dataset. As illustrated in Fig. 6, the generated sEMG signals exhibit waveform patterns and temporal dynamics that closely resemble those of the corresponding real samples. In particular, even fine-grained signal details, such as subtle fluctuations and transient peaks, are well generated, indicating that the model is capable of generating high-fidelity sEMG signals with refined structure.

### B. Extension of Dataset Coverage

To verify that our SASS strategy explicitly expands the data distribution, we conduct condition space visualization and quantitative sparsity evaluations. Specifically, we use t-SNE to project the semantic representations of the original training set, as well as those obtained through the GMSS and SASS mechanisms, into a two-dimensional space. As shown in Fig. 7, the semantic representations generated by the GMSS mechanism are evenly distributed within the original feature space, producing diverse and distribution-consistent conditions. Furthermore, the semantic representations generated by the SASS mechanism are distributed in the sparser regions of the original feature space, which significantly enlarges the coverage of the training distribution while maintaining consistency with the original data manifold.

We further verify that the samples generated under sparse condition guidance are indeed sparse in nature through quan-

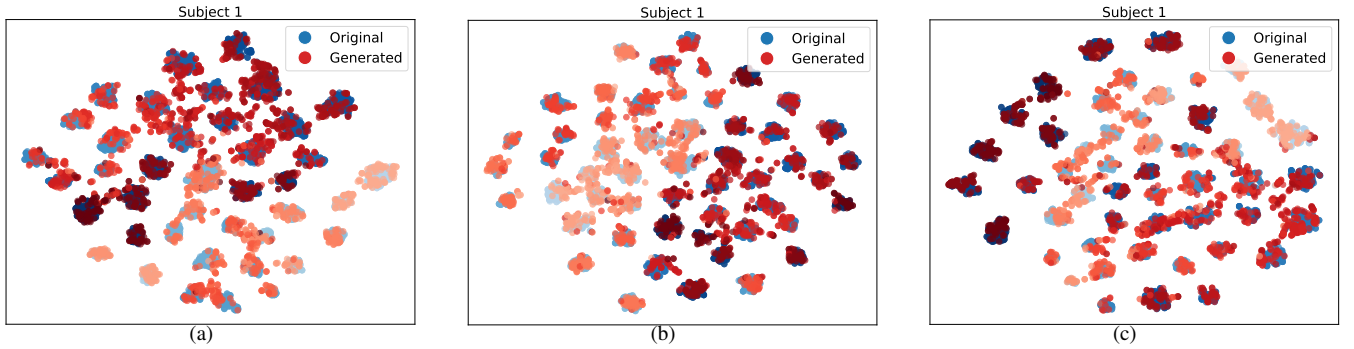


Fig. 5. Distribution visualizations of the original (blue) and generated (red) samples for subject 1 from (a) DB7, (b) DB4 and (c) DB2. Different shades of each color denote different gesture classes.

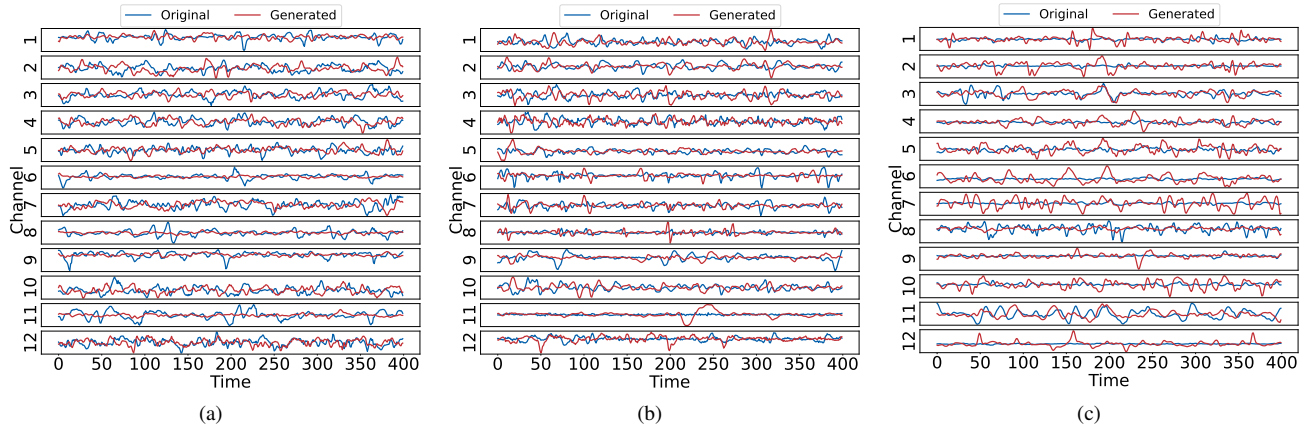


Fig. 6. Examples of original (blue) and generated (red) samples of (a) DB7, (b) DB4 and (c) DB2.

titative metrics. Specifically, following the settings in [23], [25], we adopt three sparsity measures on generated samples: the average k-nearest neighbor distance (AvgKNN), the Local Outlier Factor (LOF), and the Rarity Score. As shown in Fig. 8, the generated samples guided by the sparse conditions consistently exhibit higher AvgKNN distances, larger LOF values, and higher Rarity Scores compared to those generated by the GMSS. These results quantitatively demonstrate that the SASS mechanism successfully shifts the generated samples towards the sparse regions of the data distribution, explicitly expanding the coverage of the training manifold. This property is particularly beneficial for enhancing the generalization capability of the classifier by exposing it to more diverse and underrepresented regions of the original data space.

### C. Trade-off Between Faithfulness and Diversity

To illustrate the trade-off between faithfulness and diversity, we compare our method with three common conditional generation baselines: Label Condition, Classifier Guidance [7], and Classifier-Free Guidance [43]. The results are shown in Table VIII. The Label Condition approach introduces only coarse-grained class information, which results in relatively high FID scores (e.g., 2.77 on DB7) and low CAS scores (49.83), indicating insufficient faithfulness to the target classes. In contrast, Classifier Guidance employs an explicit classifier to steer the generation toward class-consistent samples [7], significantly improving CAS (e.g., up to 86.08) and reducing

FID. However, stronger classifier gradient guidance can overly constrain the generation process, limiting the diversity of the synthesized samples by aligning them too closely with the classifier’s decision boundaries. Classifier-Free Guidance avoids the need for an external classifier by enabling the generative model to produce both conditional and unconditional outputs during inference [43]. While it avoids the overhead of an external classifier, stronger condition strength still tends to reduce diversity by pulling generated samples toward the high-density regions of the class distribution.

Interestingly, higher faithfulness (i.e., lower FID and higher CAS) does not always translate to better downstream classification performance. For instance, although Classifier Guidance achieves the highest CAS, its accuracy on downstream tasks does not outperform the Label Condition. Our approach, SASG-DA, achieves a balanced FID and CAS while delivering consistently superior classification accuracy across multiple backbones. This demonstrates that our method effectively balances the trade-off between generating faithful and diverse samples, which is crucial for maximizing the benefit of data augmentation in downstream applications.

### D. Effectiveness in Mitigating Overfitting

To evaluate the effectiveness of our method in mitigating overfitting, we analyze the training and testing accuracy curves on randomly selected samples from DB4 and DB7. As shown in Fig. 9, the baseline model exhibits a noticeable divergence

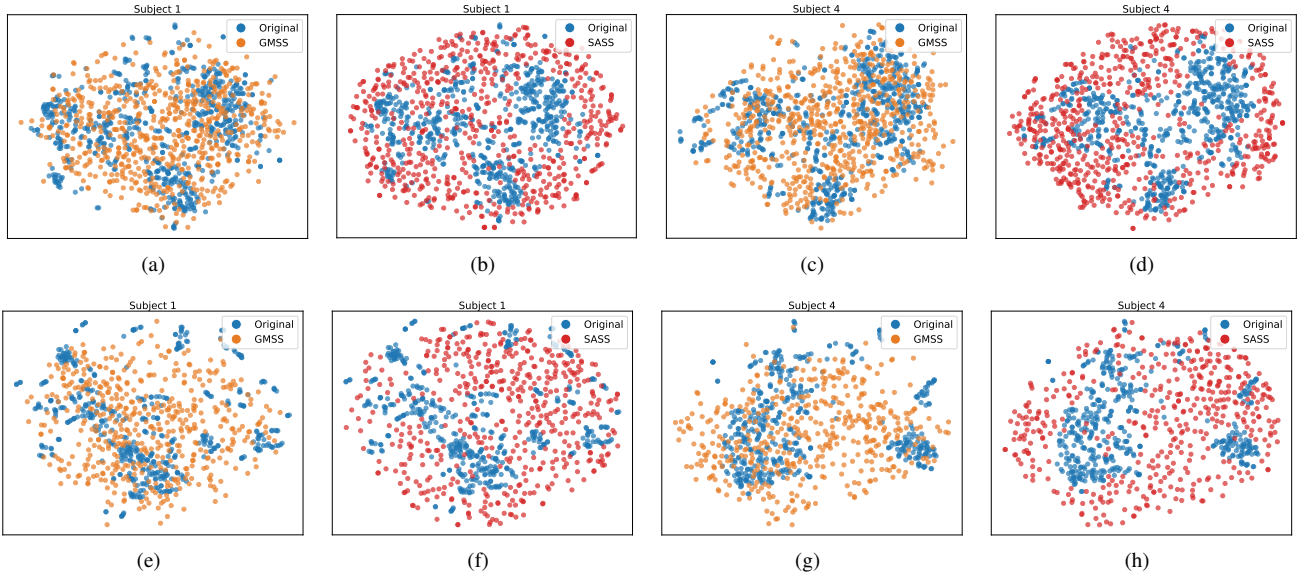


Fig. 7. Condition visualization to show the effectiveness of the SASS mechanism for subjects 1 and 4 from (a-d) DB7 and (e-h) DB4.

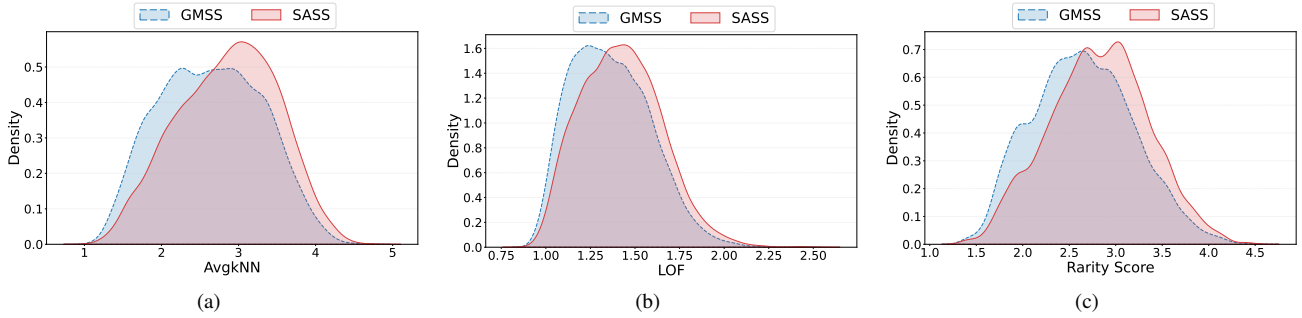


Fig. 8. Quantitative evaluation of the generated sample sparsity on DB7 using three different metrics: (a) AvgkNN, (b) LOF, and (c) Rarity Score.

TABLE VIII  
PERFORMANCE COMPARISON OF DIFFERENT GUIDANCE STRATEGIES ON DB7 AND DB4.

Method	DB7					DB4				
	FID	CAS	Crossformer	TDCT	STCNet	FID	CAS	Crossformer	TDCT	STCNet
Label Condition	2.77	49.83	80.49	77.09	80.62	2.95	45.99	68.81	66.04	68.19
Classifier Guidance	1.73	86.08	79.72	76.82	80.11	2.03	92.18	67.81	65.23	68.21
Classifier-Free Guidance	1.62	77.00	80.54	77.46	80.95	2.13	71.44	68.91	66.30	68.43
GMSS	0.88	71.73	80.87	77.57	81.67	0.87	68.09	69.44	66.99	69.41
SASG-DA	1.35	58.65	81.31	78.77	82.15	1.37	56.99	69.73	67.74	70.05

between training and testing accuracy as training progresses, indicating a tendency to overfit the training data. In contrast, our method effectively narrows the gap, demonstrating enhanced generalization and mitigated overfitting. This indicates that our data augmentation strategy enhances model generalization by providing the model with more diverse and effective samples, thereby reducing its tendency to overfit to spurious patterns or redundant data.

### E. Size and Diversity of Synthetic Data

We further explore the effect of the size and diversity of the synthetic samples on model performance. To this end, we systematically increase the size of the synthetic dataset to 1 $\times$ , 2 $\times$ , 3 $\times$ , and 4 $\times$  the size of the original training set. As shown in

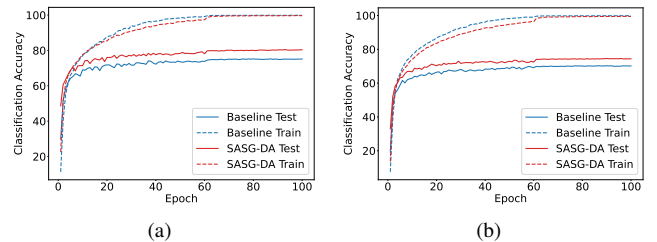


Fig. 9. Training and testing accuracy curves for randomly selected subjects from (a) DB7 and (b) DB4.

Fig. 10, experiments on both DB7 and DB4 demonstrate that the classification accuracy improves monotonically with the growth of synthetic data. Specifically, for DB7, we observe

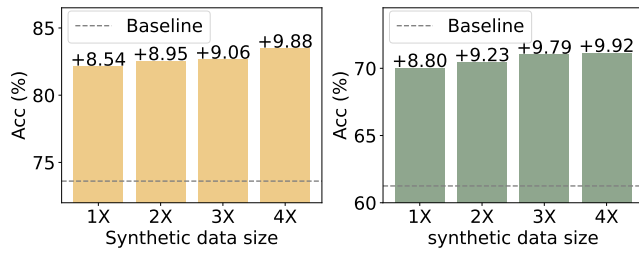


Fig. 10. Effect of synthetic data size on classification accuracy for DB7 (left) and DB4 (right).

consistent gains from +8.54% to +9.88% compared to the baseline when enlarging the synthetic set. A similar trend is seen on DB4, where the accuracy steadily rises from +8.80% to +9.92% above the baseline. These results suggest that expanding the size and diversity of synthetic samples contributes to more robust model generalization.

### F. Limitation and Future Work

Although the proposed diffusion-based augmentation method effectively improves classification performance by generating faithful and diverse samples, its generation efficiency remains a limitation [44]. Due to the iterative nature of the diffusion process, producing a large amount of synthetic data can be computationally expensive and time-consuming compared to other generative models. In future work, we plan to investigate acceleration strategies, such as distillation-based fast samplers [44], to reduce generation costs without compromising sample diversity and fidelity. Exploring lightweight diffusion architectures could further facilitate practical deployment in data augmentation applications.

## VII. CONCLUSION

Informative data scarcity and overfitting remain major challenges for deploying sEMG-based gesture recognition in real-world human-machine interaction (HMI) applications. To address these issues, we propose a novel diffusion-based data augmentation framework, SASG-DA, which integrates semantic representation guidance and sparse-aware sampling to generate both faithful and diverse training samples. By modeling and selectively sampling from a learned semantic embedding space, our method enables flexible and controllable augmentation that not only enhances class fidelity but also improves coverage of underrepresented regions. Extensive experiments on multiple public sEMG datasets demonstrate that SASG-DA consistently improves recognition accuracy and generalization over existing augmentation strategies. We believe this work provides a practical and principled data augmentation approach for improving gesture recognition performance. Moreover, the proposed framework holds promise for broader application in biosignal and time-series classification tasks where data scarcity and overfitting are common challenges. Future work will explore extending this augmentation approach to other domains where semantically conditioned and diversity-aware sample generation is beneficial.

## REFERENCES

- [1] P. Kaifosh and T. R. Reardon, "A generic non-invasive neuromotor interface for human-computer interaction," *Nature*, pp. 1–10, 2025.
- [2] J. Xu, R. Wang, S. Shang, A. Chen, L. Winterbottom, T.-L. Hsu, W. Chen, K. Ahmed, P. L. La Rotta, X. Zhu *et al.*, "Chatemg: Synthetic data generation to control a robotic hand orthosis for stroke," *IEEE Robot. Autom. Lett.*, 2024.
- [3] V. Sivakumar, J. Seely, A. Du, S. Bittner, A. Berenzweig, A. Bolarinwa, A. Gramfort, and M. Mandel, "emg2qwerty: A large dataset with baselines for touch typing using surface electromyography," vol. 37, 2024, pp. 91 373–91 389.
- [4] P. Tsinganos, B. Cornelis, J. Cornelis, B. Jansen, and A. Skodras, "Data augmentation of surface electromyography for hand gesture recognition," *Sens.*, vol. 20, no. 17, p. 4892, 2020.
- [5] V. Mendez, C. Lhoste, and S. Micera, "Emg data augmentation for grasp classification using generative adversarial networks," in *EMBC. IEEE*, 2022, pp. 3619–3622.
- [6] J. Ao, S. Liang, T. Yan, R. Hou, Z. Zheng, and J. Ryu, "Overcoming the effect of muscle fatigue on gesture recognition based on semg via generative adversarial networks," *Expert Syst. Appl.*, vol. 238, p. 122304, 2024.
- [7] P. Dhariwal and A. Nichol, "Diffusion models beat gans on image synthesis," *Proc. Adv. Neural Inf. Process. Syst.*, vol. 34, pp. 8780–8794, 2021.
- [8] B. Xiong, W. Chen, H. Li, Y. Niu, N. Zeng, Z. Gan, and Y. Xu, "Patchemg: Few-shot emg signal generation with diffusion models for data augmentation to improve classification performance," *IEEE Trans. Instrum. Meas.*, 2024.
- [9] Z. Wang, L. Wei, T. Wang, H. Chen, Y. Hao, X. Wang, X. He, and Q. Tian, "Enhance image classification via inter-class image mixup with diffusion model," in *Proc. IEEE/CVF Conf. Comput. Vis. Pattern Recognit.*, 2024, pp. 17 223–17 233.
- [10] Y. Wang and L. Chen, "Inversion circle interpolation: Diffusion-based image augmentation for data-scarce classification," in *Proc. IEEE/CVF Conf. Comput. Vis. Pattern Recognit.*, 2025, pp. 25 560–25 569.
- [11] F. Rahat, M. S. Hossain, M. R. Ahmed, S. K. Jha, and R. Ewetz, "Data augmentation for image classification using generative ai," in *IEEE/CVF Winter Conference on Applications of Computer Vision. IEEE*, 2025, pp. 4173–4182.
- [12] B. Trabucco, K. Doherty, M. A. Gurinas, and R. Salakhutdinov, "Effective data augmentation with diffusion models," in *Proc. Int. Conf. Learn. Represent.*, 2024.
- [13] A. K. N. Vu, T. Q. Truong, V.-T. Nguyen, T. D. Ngo, T.-T. Do, and T. V. Nguyen, "Multi-perspective data augmentation for few-shot object detection," in *Proc. Int. Conf. Learn. Represent.*, 2025.
- [14] J. Yang, D. Cha, D.-G. Lee, and S. Ahn, "Stcnct: Spatio-temporal cross network with subject-aware contrastive learning for hand gesture recognition in surface emg," *Comput. Biol. Med.*, vol. 185, p. 109525, 2025.
- [15] M. A. Al-Qaness and S. Ni, "Tcnn-kan: Optimized cnn by kolmogorov-arnold network and pruning techniques for semg gesture recognition," *IEEE J. Biomed. Health Inform.*, 2024.
- [16] Z. Wang, J. Yao, M. Xu, M. Jiang, and J. Su, "Transformer-based network with temporal depthwise convolutions for semg recognition," *Pattern Recogn.*, vol. 145, p. 109967, 2024.
- [17] K. Zhao, Z. He, A. Hung, and D. Zeng, "Dominant shuffle: A simple yet powerful data augmentation for time-series prediction," *arXiv preprint arXiv:2405.16456*, 2024.
- [18] C. Cao, F. Zhou, Y. Dai, J. Wang, and K. Zhang, "A survey of mix-based data augmentation: Taxonomy, methods, applications, and explainability," *ACM Comp. Surv.*, vol. 57, no. 2, pp. 1–38, 2024.
- [19] J. J. Bird, M. Pritchard, A. Fratini, A. Ekárt, and D. R. Faria, "Synthetic biological signals machine-generated by gpt-2 improve the classification of eeg and emg through data augmentation," *IEEE Robot. Autom. Lett.*, vol. 6, no. 2, pp. 3498–3504, 2021.
- [20] K. Islam, M. Z. Zaheer, A. Mahmood, and K. Nandakumar, "Diffusemix: Label-preserving data augmentation with diffusion models," in *Proc. IEEE/CVF Conf. Comput. Vis. Pattern Recognit.*, 2024, pp. 27 621–27 630.
- [21] Z. Li, L. Chen, J. Andrews, Y. Ba, Y. Zhang, and A. Xiang, "Gendataagent: On-the-fly dataset augmentation with synthetic data," in *Proc. Int. Conf. Learn. Represent.*, 2025.

- [22] S. Sadat, J. Buhmann, D. Bradley, O. Hilliges, and R. M. Weber, "Cads: Unleashing the diversity of diffusion models through condition-annealed sampling," in *Proc. Int. Conf. Learn. Represent.*, 2024.
- [23] V. Schwag, C. Hazirbas, A. Gordo, F. Ozgenel, and C. Canton, "Generating high fidelity data from low-density regions using diffusion models," in *Proc. IEEE/CVF Conf. Comput. Vis. Pattern Recognit.*, 2022, pp. 11 492–11 501.
- [24] J. C. Ye, S. Um *et al.*, "Don't play favorites: Minority guidance for diffusion models," in *Proc. Int. Conf. Learn. Represent.* International Conference on Learning Representations, 2024.
- [25] S. Um and J. C. Ye, "Self-guided generation of minority samples using diffusion models," in *Proc. Eur. Conf. Comput. Vis.* Springer, 2024, pp. 414–430.
- [26] —, "Minority-focused text-to-image generation via prompt optimization," in *Proc. IEEE/CVF Conf. Comput. Vis. Pattern Recognit.*, 2025, pp. 20 926–20 936.
- [27] J. Ho, A. Jain, and P. Abbeel, "Denoising diffusion probabilistic models," *Proc. Adv. Neural Inf. Process. Syst.*, vol. 33, pp. 6840–6851, 2020.
- [28] X. Yuan and Y. Qiao, "Diffusion-ts: Interpretable diffusion for general time series generation," in *Proc. Int. Conf. Learn. Represent.*, 2024.
- [29] J. Han, H. Choi, Y. Choi, J. Kim, J.-W. Ha, and J. Choi, "Rarity score: A new metric to evaluate the uncommonness of synthesized images," in *Proc. Int. Conf. Learn. Represent.*, 2024.
- [30] M. Atzori, A. Gijsberts, C. Castellini, B. Caputo, A.-G. M. Hager, S. Elsig, G. Giatsidis, F. Bassetto, and H. Müller, "Electromyography data for non-invasive naturally-controlled robotic hand prostheses," *Sci. Data*, vol. 1, no. 1, pp. 1–13, 2014.
- [31] S. Pizzolato, L. Tagliapietra, M. Cognolato, M. Reggiani, H. Müller, and M. Atzori, "Comparison of six electromyography acquisition setups on hand movement classification tasks," *PLoS ONE*, vol. 12, no. 10, p. e0186132, 2017.
- [32] A. Krasoulis, I. Kyranou, M. S. Erden, K. Nazarpour, and S. Vijayakumar, "Improved prosthetic hand control with concurrent use of myoelectric and inertial measurements," *J Neuroeng Rehabil*, vol. 14, no. 1, p. 71, 2017.
- [33] M. Heusel, H. Ramsauer, T. Unterthiner, B. Nessler, and S. Hochreiter, "Gans trained by a two time-scale update rule converge to a local nash equilibrium," *Proc. Adv. Neural Inf. Process. Syst.*, vol. 30, 2017.
- [34] M. M. Breunig, H.-P. Kriegel, R. T. Ng, and J. Sander, "Lof: identifying density-based local outliers," in *Proc. ACM SIGMOD Int. Conf. Manag. Data*, 2000, pp. 93–104.
- [35] Y. Zhang and J. Yan, "Crossformer: Transformer utilizing cross-dimension dependency for multivariate time series forecasting," in *Proc. Int. Conf. Learn. Represent.*, 2023.
- [36] T. T. Um, F. M. Pfister, D. Pichler, S. Endo, M. Lang, S. Hirche, U. Fietzek, and D. Kulić, "Data augmentation of wearable sensor data for parkinson's disease monitoring using convolutional neural networks," in *Proc. ACM Int. Conf. Multimodal Interaction*, 2017, pp. 216–220.
- [37] A.-A. Semoglou, E. Spiliotis, and V. Assimakopoulos, "Data augmentation for univariate time series forecasting with neural networks," *Pattern Recogn.*, vol. 134, p. 109132, 2023.
- [38] M. Chen, Z. Xu, A. Zeng, and Q. Xu, "Fraug: Frequency domain augmentation for time series forecasting," *arXiv preprint arXiv:2302.09292*, 2023.
- [39] A. M. Aboussalah, M. Kwon, R. G. Patel, C. Chi, and C.-G. Lee, "Recursive time series data augmentation," in *Proc. Int. Conf. Learn. Represent.*, 2023.
- [40] H. Zhang, M. Cisse, Y. N. Dauphin, and D. Lopez-Paz, "mixup: Beyond empirical risk minimization," in *Proc. Int. Conf. Learn. Represent.*, 2018.
- [41] X. Zhang, R. R. Chowdhury, J. Shang, R. Gupta, and D. Hong, "Towards diverse and coherent augmentation for time-series forecasting," in *Proc. IEEE Int. Conf. Acoust. Speech Signal Process.* IEEE, 2023, pp. 1–5.
- [42] H. Ryu, S. Yoon, H. S. Yoon, E. Yoon, and C. D. Yoo, "Simpsti: A simple strategy to preserve spectral information in time series data augmentation," in *Proc. AAAI Conf. Artif. Intell.*, vol. 38, no. 13, 2024, pp. 14 857–14 865.
- [43] J. Ho and T. Salimans, "Classifier-free diffusion guidance," in *Proc. Adv. Neural Inf. Process. Syst. Workshop*, 2021.
- [44] T. Yin, M. Gharbi, R. Zhang, E. Shechtman, F. Durand, W. T. Freeman, and T. Park, "One-step diffusion with distribution matching distillation," in *Proc. IEEE Conf. Comput. Vis. Pattern Recognit.*, 2024, pp. 6613–6623.